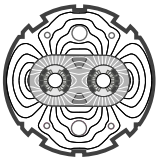

LHC Project Note 203

October 8, 1999

Measurements of Complex Permeability and Permittivity of Ferrites for the LHC Injection Kicker

Fritz Caspers, Michele Morvillo, Carlota Gonzalez, CERN
and Misha D'yachkov, TRIUMF

Keywords: permeability, permittivity, microwave measurements, impedance, kicker

Summary

The LHC injection kicker is made by a lumped element delay line using capacitors and single turn inductors. For these inductors different types of ferrites (Philips 8C11 and 4A4) are considered. At the time when this report was written only 4A4 ferrite was available for a prototype kicker construction, as well as for impedance measurements by the wire method. The 4A4 ferrite comes in standard blocks (42 x 54 x 74 mm) which are quite expensive, so there were virtually no spare blocks available which could be machined for use in the standard coaxial technique. Thus we have developed a strip-line test jig which permits testing material parameters on existing ferrite blocks without additional (destructive) machining. Special aspects, advantages and difficulties of this method are discussed. The bench measurements and also theoretical and numerical estimates of the beam coupling impedance of the kickers are under way.

1 Introduction

In the course of investigation of the impedance of the LHC injection kicker it was necessary to identify parameters of the material to be used in the kicker in the frequency range up to 1 GHz. It turned out in the beginning of the work that the frequency dependency of the permittivity and permeability of the ferrite material (namely 4A4) available from the manufacturer were rather incomplete, so it was decided to provide a locally available test method.

The complex relative dielectric constant $\epsilon = \epsilon$' - jϵ" and the complex permeability $\mu = \mu$'-jμ" of a given ferrite material are both a function of frequency and define the electric and magnetic losses of the material under consideration. There are many ways to measure these quantities (which are usually defined for small signal excitation only).

The basic concept for measuring permittivity is to have a sample of suitable shape that can be exposed to a nearly pure electric field (e.g. to be placed into a capacitor which has linear dimensions very small compared to a quarter of a free space wavelength of the highest frequency of interest). In this case the errors due to the magnetic properties can be neglected to a high degree of accuracy.

The equivalent concept for magnetic measurements is a torus-like shaped sample of sufficiently small size. When going towards higher frequencies the lumped element methods mentioned above approach their limit of validity and are replaced with traveling or standing wave techniques. A well known technique is to place a toroidal sample of the material into a coaxial line and measure the reflection and transmission coefficients (S_{11} and S_{21}) of this structure. The S-paramater is related to the term scattering. S_{11} is defined as a complex voltage ratio of reflected vs. incident wave at port No. 1 of some device under test (DUT). S_{21} is the transmission from port No. 1 to port No. 2 of some DUT and also defined as the complex ratio of transmitted vs. incident wave.

This wide-band technique gives good results if the sample length is in a reasonable relation to the wavelength at center frequency. However the accuracy in terms of loss factor for low loss material is rather poor and for high precision loss factor measurements on low loss materials normally resonator techniques should be used instead.

Finally for very high frequencies (> 10 GHz) which would require an extremely small sample size even for a guided traveling wave method (line dimensions limited by higher order modes), free space traveling (and standing) wave techniques are in use.

2 Permeability and permittivity

A general method of measuring the complex permeability (μ) and permittivity (ϵ) from the complex S-parameters uses circular coaxial lines and requires toroidal samples of the ferrite material with very tight mechanical tolerances. The theory and the analysis of this technique can be found in [1].

More recently an alternative implementation of this method using a strip-line transmission line in which specially machined blocks of the material which has to be tested can be easily inserted has been described in [2]. In that paper an automated vector network analyzer was used to perform swept frequency S-parameter measurements on a loaded stripline fixture. The complex ϵ and μ are then calculated from the measured S-parameters S_{11} and S_{21}.

3 Theory

Let us consider a transmission line of total length $L = t + 2l$ in which the sample of material of length t and unknown complex permittivity and permeability

$$\begin{aligned} \epsilon &= \epsilon' - j\epsilon'', \\ \mu &= \mu' - j\mu'' \end{aligned} \tag{1}$$

is placed exactly in the middle (Fig. 1). First we assume that the transmission line has exactly the same characteristic impedance as the cables (this will simplify the derivation of

the formulae).

If Z_0 is the characteristic impedance of the stripline in a free space, then the characteristic impedance of the stripline filled with the material with relative permittivity ϵ and permeability μ becomes:

$$Z = Z_0\sqrt{\frac{\mu}{\epsilon}}. \tag{2}$$

The propagation constant in the region where there is no ferrite is $k_0 = \omega\sqrt{\mu_0\epsilon_0} = \omega/c$, where c is the speed of light in vacuum. The propagation constant k in the region with the ferrite is usually complex

$$k = k_0\sqrt{\mu\epsilon}. \tag{3}$$

The reflection and transmission parameters can be written as [3]

$$\begin{aligned} S_{11} &= \frac{R(1-T^2)}{1-T^2R^2} \\ S_{21} &= \frac{T(1-R^2)}{1-T^2R^2} \end{aligned} \tag{4}$$

where T is the "transmission" coefficient of the filled line where t is the length of the sample

$$T = e^{-jkt} \tag{5}$$

and R is the "reflection" coefficient for the vacuum-material interface

$$R = \frac{Z - Z_0}{Z + Z_0}. \tag{6}$$

We can rewrite the R as

$$R = \frac{\sqrt{\frac{\mu}{\epsilon}} - 1}{\sqrt{\frac{\mu}{\epsilon}} + 1}. \tag{7}$$

Using Eqs. 2-6, one can find the expressions for ϵ and μ expressed in terms of R and k

$$\begin{aligned} \epsilon &= \frac{k}{k_0}\left(\frac{1-R}{1+R}\right) \\ \mu &= \frac{k}{k_0}\left(\frac{1+R}{1-R}\right) \end{aligned} \tag{8}$$

which can be found from the measured values of S_{21} and S_{11}

$$\begin{aligned} kt &= cos^{-1}\left(\frac{\delta^2 + S_{21}^2 - S_{11}^2}{2\delta S_{21}}\right) \\ R &= \frac{S_{11}}{\delta - S_{21}\, e^{-jkt}} \end{aligned} \tag{9}$$

where $\delta = \exp(-jk_0 2l)$ is the delay in the parts of the stripline not filled with the material ($2l$ is the total length of those parts).

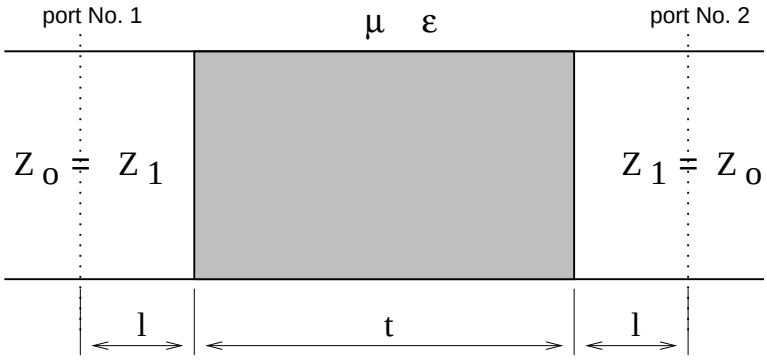

Figure 1: Simplified circuit diagram for determination of S-parameters.

4 Experimental Setup

As it has been noted above we could not use a standard technique and machine toroidal samples out of the ferrite, which was available in blocks, and therefore we have developed a different non-distructive technique. We have built the strip-line transmission line in such a way that 4 blocks of ferrite could completely fill the empty space between the outer and the central conductors (see Fig. 2).

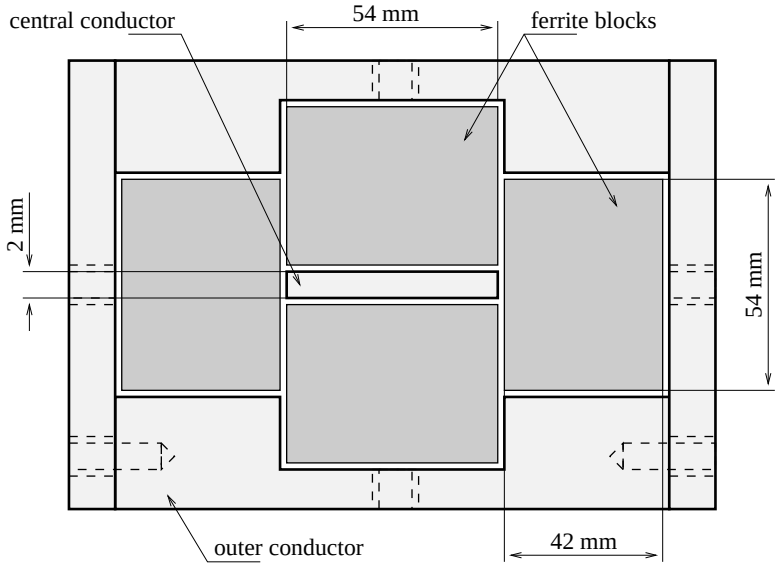

Figure 2: Cross-section of the jig filled with ferrite.

Ideally, the characteristic impedance of the stripline should be made as close as possible to the one of the cables (in our case it is 50 Ohm), but in our circumstances, this was impossible to achieve, and the impedance of our stripline was about 30% higher than the impedance of the cables. So we had to derive new formulae to take into account the effect of the mismatch between the cables and the stripline. We have also taken into account the fact that the ferrite sample may be placed not exactly in the middle of the jig (in some of our measurements the blocks of ferrite were placed closer to one end of the jig than to

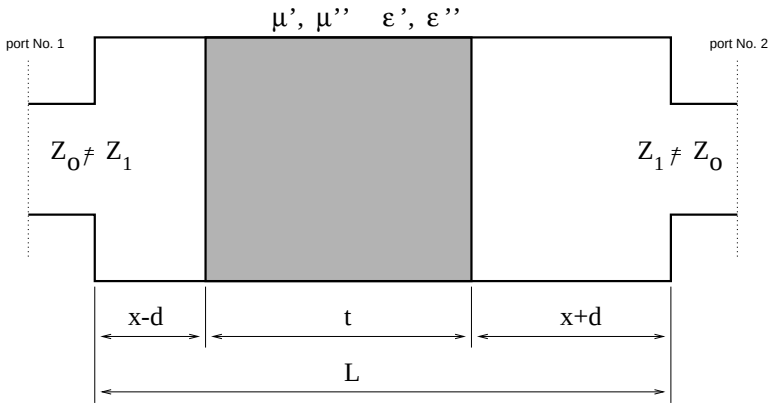

Figure 3: Diagram for determining S-parameters in general case.

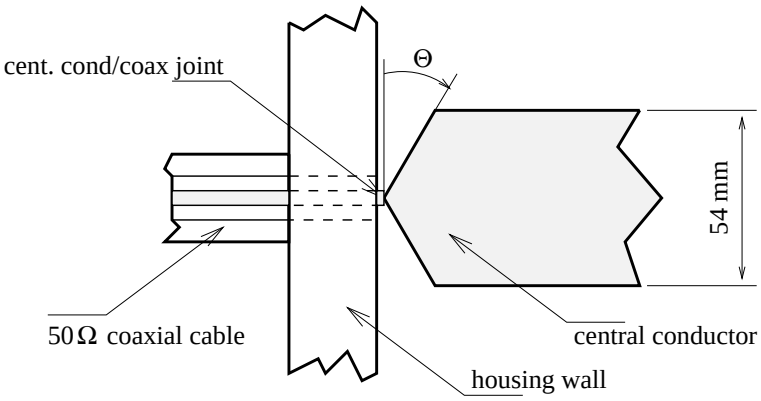

Figure 4: Coax to central electrode connection.

another). The diagram used in our analysis is shown on Fig. 3. The resulting formulae are quite long to be presented here in the report, instead we have written a small computer code to evaluate these expressions.

The measurement settings are quite sensitive to the air gaps between the ferrite blocks, therefore teflon screws on each side of the outer conductor were used to hold the blocks together and to ensure that there are no gaps between them.

Special care has been taken to obtain the best possible transition between the stipline and the central electrode. This has been achieved by tapering the corners of the central electrode (see Fig. 4). The optimal angles has been found empirically in a series of iterations by cutting the strip at bigger angle until the reflection has become reasonably small. It has been found that $\theta \approx 10^o$ gives the best results.

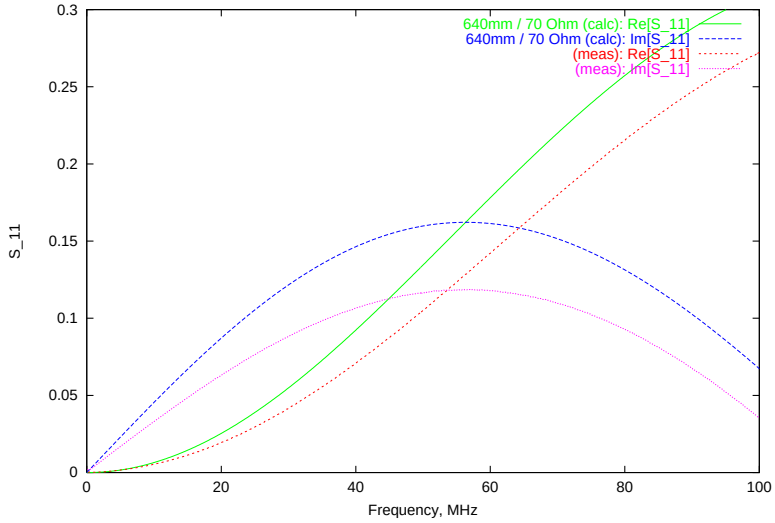

Figure 5: S_{11} vs. frequency of an empty jig calculated assuming a characteristic impedance of the jig $Z_1 = 70\ \Omega$ ($Z_0 = 50\ \Omega$) and the length $L = 640$ mm.

5 Results

5.1 S_{11} measurements for an empty test jig

In order to find the values of the characteristic impedance of the transmission line and its length we measured the S_{11} coefficient for an empty transmission line and compared the results with the values calculated using the theoretical model. As one can see from Figs. 5 and 6 the best fit was achieved when the value of the characteristic impedance of the empty line was 65 Ω and the total length of the device was L = 680 mm. This fits reasonably well to the total mechanical length of the jig between the cable ports. The characteristic impedance of the empty jig, however, calculated directly from the S_{11} parameter displayed in time domain (see Fig. 18) should be slightly higher: 68.5 Ω. This may be due to the fact that we have not included the parasitic capacitance localized at the point where the cable is connected to the central conductor (Fig. 4). One can clearly see the bump on the S_{11} graph (Fig. 18) near the "zero" time delay (the point where the cable is connected to the jig). We can use this data to estimate that the parasitic capacitance at the joint is about 5pF.

5.2 Measurements with the Ferrite

In the next set of measurements the stripline has been filled with the ferrite and then the S-paramaters have been measured. As it has already been mentioned above, in order to implement that method one has to measure at least two S-parameters (e.g. S_{21} and S_{11}) for each frequency for which we are interested to determine μ and ϵ. Thus from two complex S-parameters (S_{11} and S_{12}) we can determine the two complex unknowns μ and ϵ independently.

The 8C11 ferrite which will be used in the LHC injection kicker was unavailable at the time this note was written, therefore the measurements have been performed only for 4A4

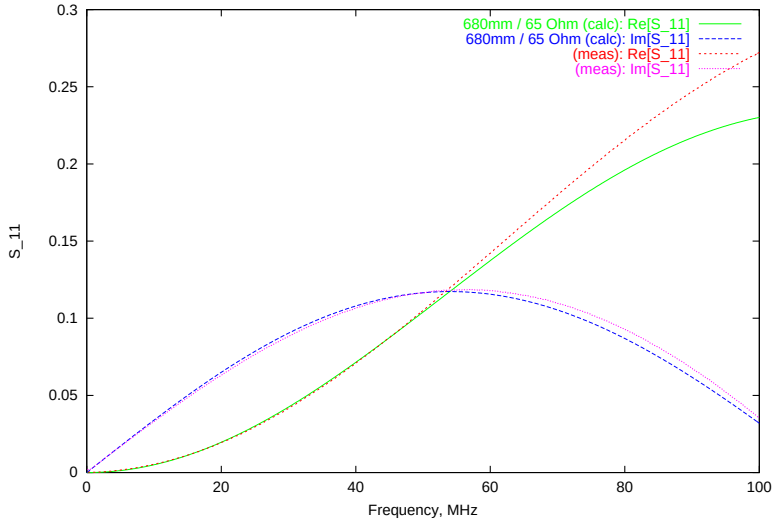

Figure 6: S_{11} vs. frequency of an empty jig calculated assuming the impedance of the jig $Z_1 = 65\ \Omega$ ($Z_0 = 50\ \Omega$) and the length $L = 680$ mm.

(it was incorrectly assumed at the time that these materials should have similar electric and magnetic properties). The measurements have been done for three different lengths of the ferrite sample: 1 x 74 mm, 2 x 74 mm and 8 x 74 mm. The results of the measurements are presented at the end of the report. The results for the 8 x 74 mm sample (Figs. 11-14) are shown for illustration purpose only, as one can see that with such a long sample we cannot measure S_{21} beyond 20 MHz. Using the shorter samples (minimum length in our case was 74 mm), however, we can increase the range up to 100-200 MHz.

5.3 Permittivity and Permeability below 200 kHz

At very low frequencies, where the quasistatic approximations are valid, μ and ϵ can be determined from a single lumped element model. In one case we consider our ferrite filled jig as an inductor by putting a short circuit at port No. 2 and measure the input impedance at port No. 1. The maximum frequency up to which this method can work is given by the rule that the maximum linear dimension of the device under test should be less than 10% of the quarter wavelength. In our case we have to consider the free-space wavelength to be divided by $\sqrt{\mu\,\epsilon}$. In analogy, we can measure the capacitance at port No. 1, by leaving port No. 2 open. We have measured this way for the completely filled test jig an inductance L=101 μH at 1 kHz (measured with LCR-meter) and L=97 μH at 200 kHz (measured with the network analyzer). Assuming a characteristic impedance of 68.5 Ω for the empty stripline (jig) we can deduce the μ' value to be about 660 at the frequencies mentioned above. In a similar way (port No. 2 open) we have seen a strong increase in ϵ from 15 (at 100 Khz) to 50 (at 1 kHz), this was slightly lower than indicated in Philips tables, but it can be easily attributed to the presence of a radial airgap in our test jig. Since the ferrite blocks with precisely machined surfaces were tightly pushed together by nylon screws, we believe that the effect of a potential azimuthal airgap between the ferrite blocks (effecting μ values) can be neglected.

5.4 Permittivity and Permeability above 200 kHz

Using the formulae derived above and plugging there the parameters for the characteristic impedance and the length found from measurements done on the empty jig, we can find the permittivity and permeability of the ferrite samples and compare the results with the data provided by Philips. The results of our calculations of permeability for the shorter sample (1 x 74 mm) are shown in Figs. 15 and for the longer one (2 x 74) in Figs. 16. The real and imaginary parts of permittivity for both 1 x 74 mm and 2 x 74 mm samples are shown in Fig. 17.

6 Discussion

It has been suggested in [2] that in order to avoid dimensional resonances in the material one has to ensure that its length $t < \lambda_m/2$ (where λ_m is the wavelength inside the material). We have observed, however, that the agreement between the Philips data and our measurements is reasonably good even when this condition is not met (e.g. see Figs. 16 and 17).

The algorithm we use to recover the permittivity and permeability from the measured S-parameters requires that the transition between the cable and the jig be smooth enough, in order to avoid localized capacitance or inductance at the transition point. However, as we can see from Fig. 18 it is not true in our case. Another technique [4] would be better suited for structures which may have significant imperfections (in our case it is the point of coax to the jig connection). That technique requires a different experimental set-up and cannot be applied for the analysis of our data. We should keep in mind that a typical permittivity of this type of ferrite is 10-12 and has a very strong impact on the penetration depth (skin-depth) of this ferrite. This length is defined as the length at which the field decays by 8.6 dB. Calculated data for the propagation attenuation and S_{21} (which are about equal for strong damping) with the same complex μ for the 4A4-type material, but different values of ϵ, are shown in Fig. 19.

7 Conclusion

The technique described in this report is similar to the traditional one, but it does not require to specially machine the samples in order to fit them in a given cross-section of the stripline/coaxial transmission line, instead the stripline is tailored to match the shape of the samples.

The main advantage of the technique is its non-distructive nature, i.e. the ferrite samples do not have to be machined or destroyed during measurements, but this, however, also results in some limitations of the technique. The ferrite samples used in the studies allowed us to measure real and imaginary components of permittivity and permeability of the material up to about 100 MHz (the maximum frequency range is limited by the sample length).

The values of the permittivity and permeability obtained from the measurements are in reasonably good agreement with the data provided by Philips for this type of ferrites, especially in the frequency range above 20 MHz, therefore we can use the Philips data to obtain scattering parameters and impedances in the frequency range up to 1 GHz. Below 20

MHz we observe considerable deviations from the Philips data. These deviations are at the limit of scatter of one production cycle to another and thus we cannot definitely say that the ferrite which was tested is identical to 4A4-type or probably a modified 4A4-type version.

8 Acknowledgements

We would like to thank Francesco Ruggiero, Roland Garoby and Gerhard Schröder for support and many helpful discussions, as well as Jean-Claude Guillot and Joel Gilbert Bertin for their help and patience in preparing all mechanical pieces required.

References

[1] W. B. Weir, *Automatic Measurement of Complex Dielectric Constant and Permeability at Microwave Frequencies*, Proc. IEEE, vol. 62, p.33, Jan 1974.

[2] W. Barry, *A Broad-Band, Automated, Stripline Technique for Simultaneous Measurement of Complex Permittivity and Permeability* IEEE Trans, vol. MIT-34, no. 1, p. 80, Jan. 1986.

[3] R. E. Colin, *Field Theory of Guided Waves* McGraw-Hill, New York, 1960.

[4] Michael D. Janezic, IEEE Microwave and Guided Wave Letters, Vol. 9, No. 2, Feb. 1999, pp.76-78.

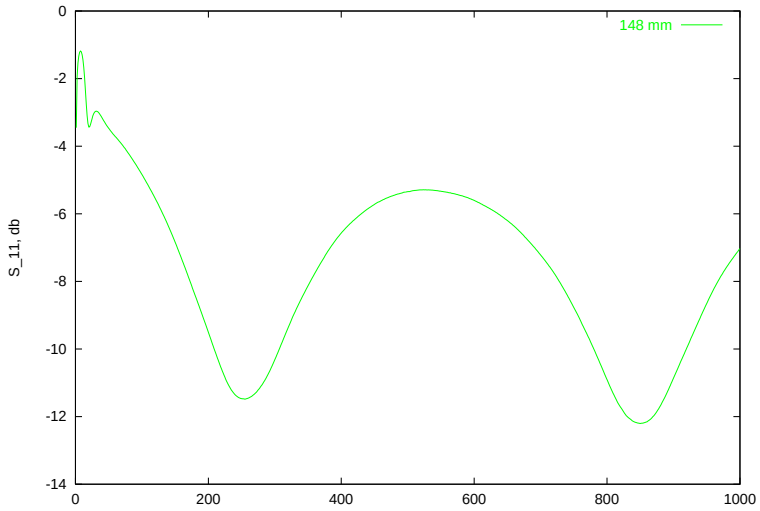

Figure 7: S_{11} amplitude measured when 2 x 4 blocks were in the jig (total length of the ferrite $t = 148$ mm).

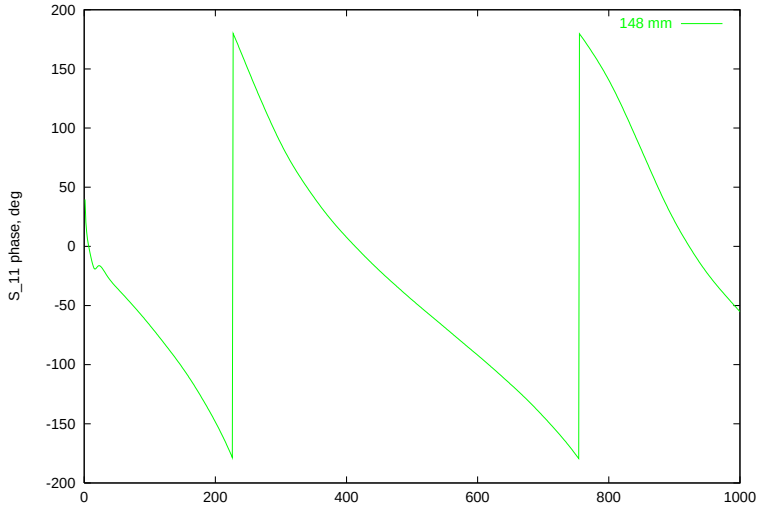

Figure 8: S_{11} phase for 2 x 4 blocks were in the jig (total length of the ferrite $t = 148$ mm).

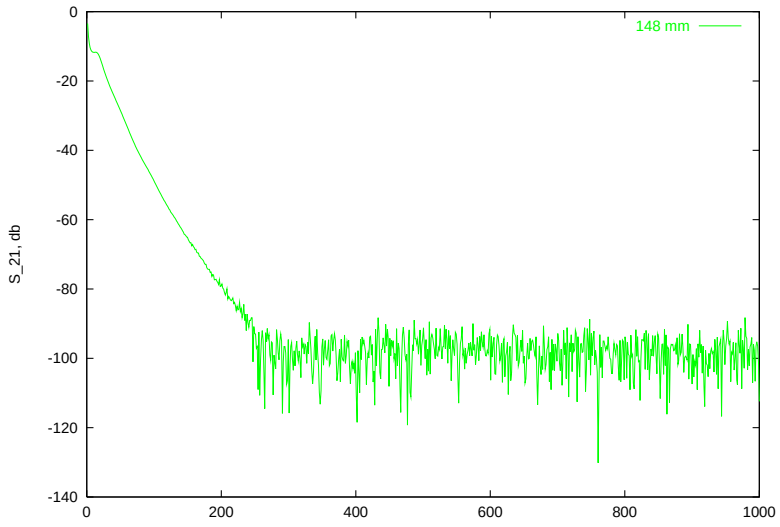

Figure 9: S_{21} amplitude measured when 2 x 4 blocks were in the jig (total length of the ferrite $t = 148$ mm).

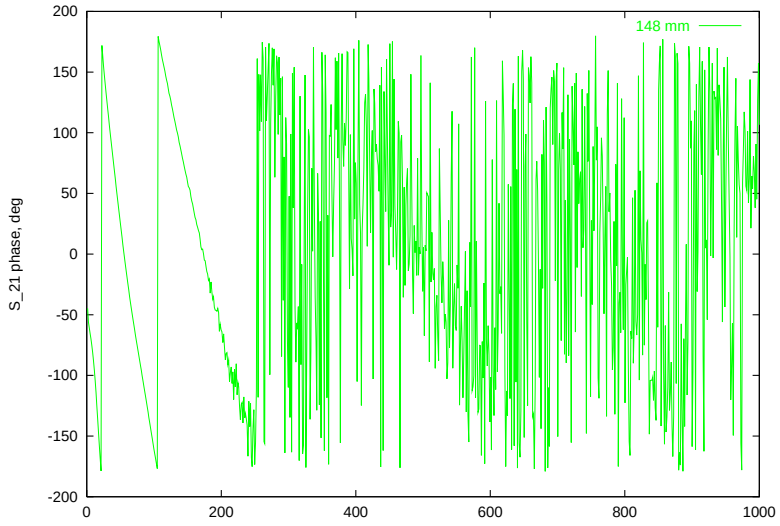

Figure 10: S_{21} phase for 2 x 4 blocks were in the jig (total length of the ferrite $t = 148$ mm).

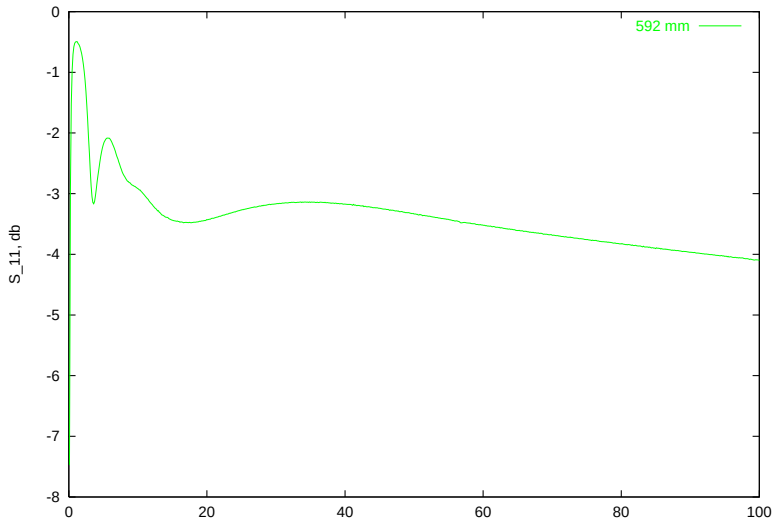

Figure 11: S_{11} amplitude measured when 8 x 4 blocks were in the jig (total length of the ferrite $t = 592$ mm).

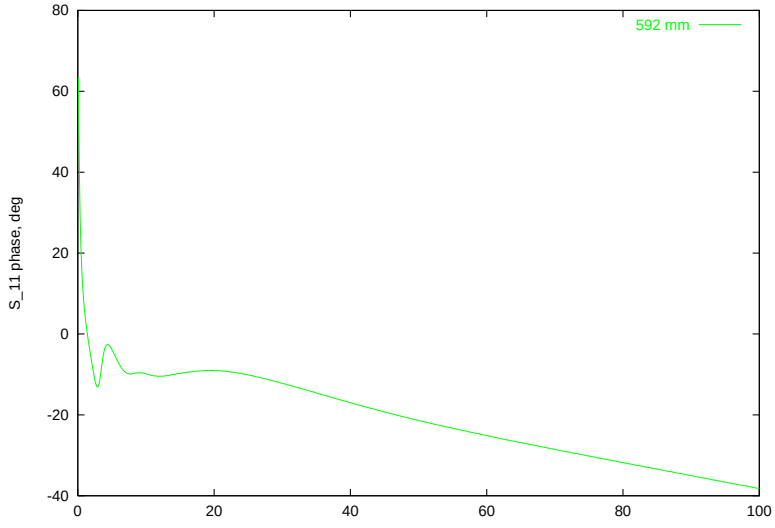

Figure 12: S_{11} phase for 8 x 4 blocks were in the jig (total length of the ferrite $t = 592$ mm).

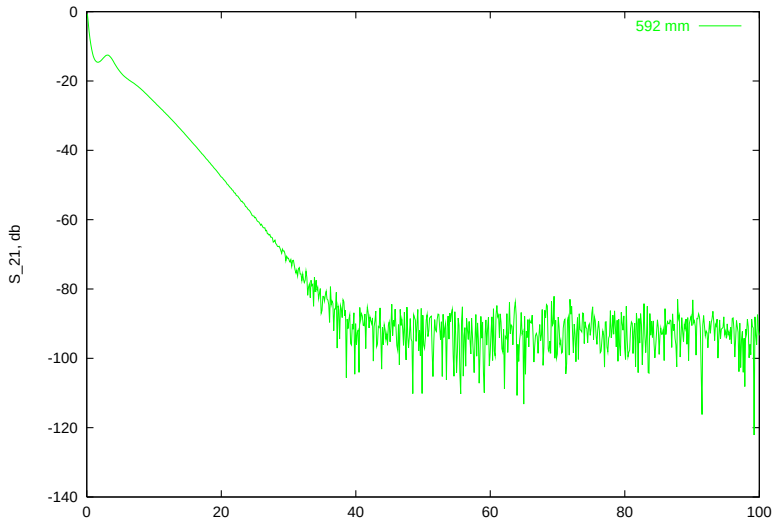

Figure 13: S_{21} amplitude measured when 8 x 4 blocks were in the jig (total length of the ferrite $t = 592$ mm).

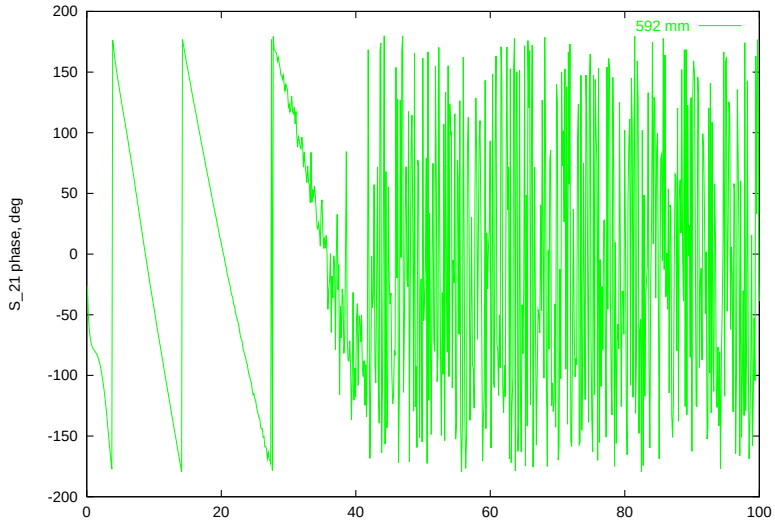

Figure 14: S_{21} phase for 8 x 4 blocks were in the jig (total length of the ferrite $t = 592$ mm).

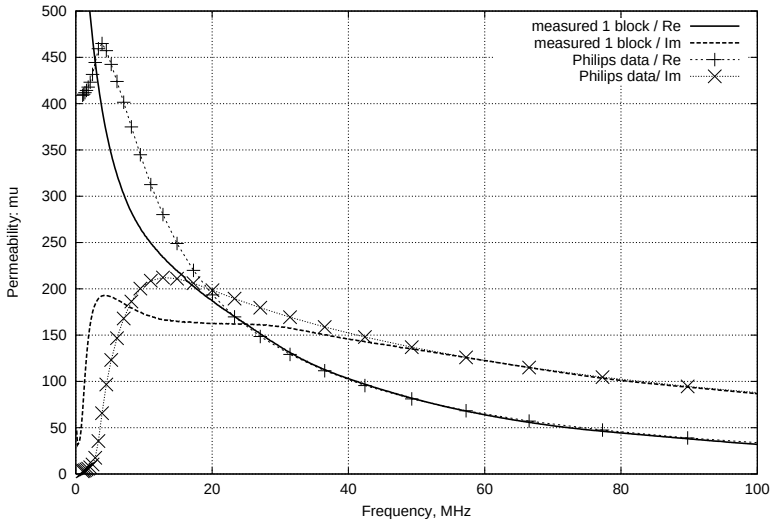

Figure 15: Permeability μ calculated from the measured S-parameters. $Z = 65\ \Omega$ ($Z_0 = 50\ \Omega$), $L = 680$ mm, $t = 74$ mm (1 x 74 mm).

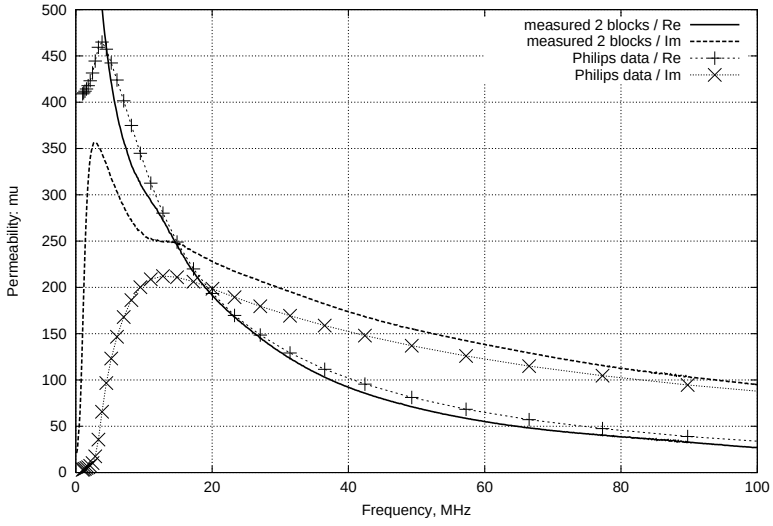

Figure 16: Permeability μ calculated from the measured S-parameters. $Z_1 = 65\ \Omega$ ($Z_0 = 50\ \Omega$), $L = 680$ mm, $t = 148$ mm (2 x 74 mm).

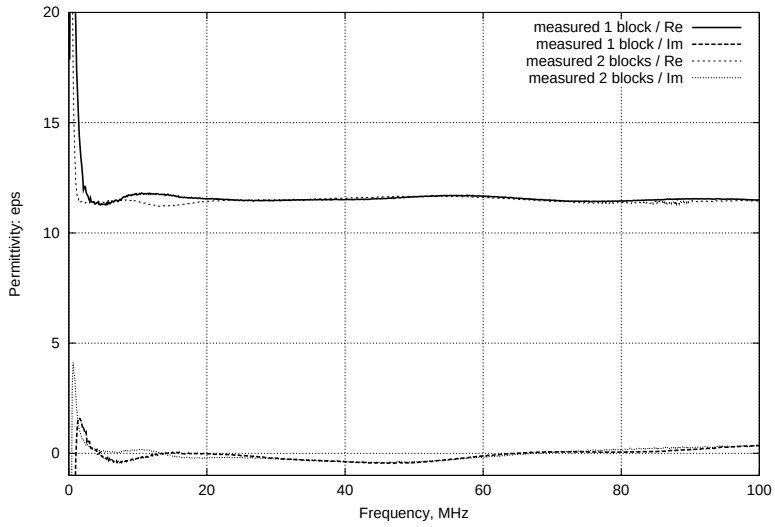

Figure 17: Permittivity ϵ calculated from the measured S-parameters.

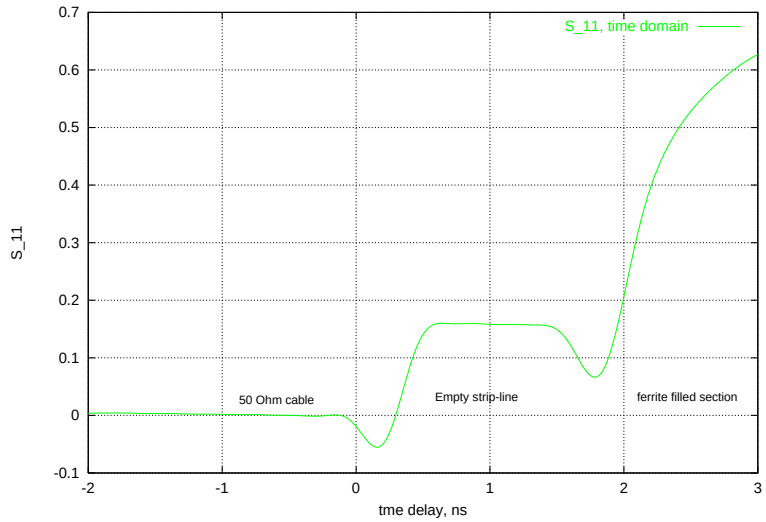

Figure 18: S_{11} parameter in time domain display (via FFT from frequency domain measurements). The bump near the zero mark indicates that there is a small capacitance (estimated to be about 5pF from the hight of the bump) at the point were the cables are connected to the jig.

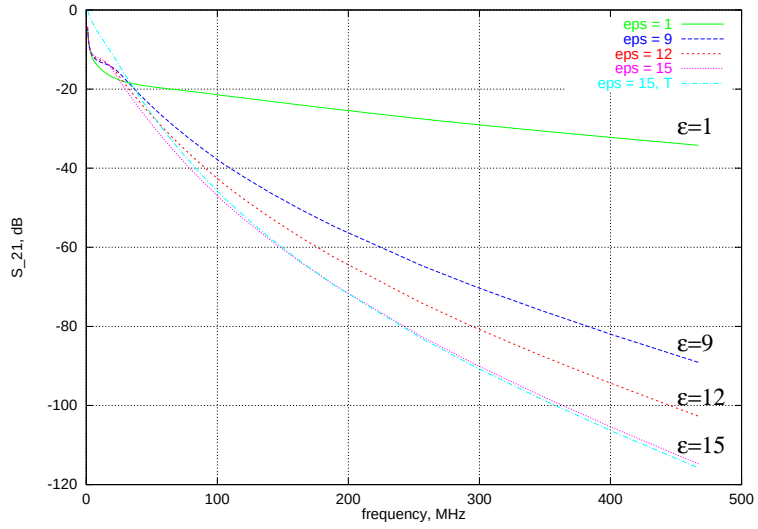

Figure 19: S_{21} parameters calculated from the Philips data for μ (4A4-type ferrite), but different values of ϵ. The transmission coefficient T (Eqn. 5) is shown for the $\epsilon = 15$.